

Figure 3. Molar volume isotherms at 613 K; unit: $\text{cm}^3 \text{ mol}^{-1}$. The numerical data on pure melts are designated in parentheses.

Acknowledgment

We express our sincere gratitude to Mr. M. Misawa for assistance in measuring the molar volumes.

Glossary

- | | |
|------------|--|
| V_m | molar volume, $\text{cm}^3 \text{ mol}^{-1}$ |
| a_n, b_n | smoothed parameters in the empirical equations |

x, y, z mole fractions of components in binary systems
 X, Y, Z mole fractions of components in ternary systems
 T absolute temperature, K

Greek Letters

σ standard errors of the molar volume equations, $\text{cm}^3 \text{ mol}^{-1}$

Registry No. NaNO_3 , 7631-99-4; KNO_3 , 7757-79-1; NaNO_2 , 7632-00-0.

Literature Cited

- (1) Janz, G. J.; Krebs, U.; Siegenthaler, H. F.; Tomkins, R. P. T. *J. Phys. Chem. Ref. Data* 1972, 7, 581.
- (2) Kamimoto, M.; Sakuta, K.; Ozawa, T.; Sakamoto, R. *Circ. Electrotech. Lab.* 1978, No. 196, 10.
- (3) Hamaguchi, H.; Kuroda, R.; Endo, S. *Jpn. Anal.* 1958, 7, 409.
- (4) Morey, G. W. "The Properties of Glass", 2nd ed.; Reinhold: New York, 1954; p 275.
- (5) Janz, G. J.; Dampier, F. W.; Lakshminarayanan, G. R.; Lorenz, P. K.; Tomkins, R. P. T. *Natl. Stand. Ref. Data Ser. (U.S. Natl. Bur. Stand.)* 1988, 15, 86-88.
- (6) Janz, G. J. *J. Phys. Chem. Ref. Data* 1980, 9, 791.
- (7) Carmichael, N. R.; Flengas, S. N. *J. Electrochem. Soc.* 1979, 126, 2098.
- (8) Odawara, O.; Okada, I.; Kawamura, K. *J. Chem. Eng. Data* 1977, 22, 222.

Received for review July 30, 1984. Accepted December 10, 1984.

Supplementary Material Available: All of the original data on the molar volume of molten $\text{NaNO}_3\text{-KNO}_3\text{-NaNO}_2$ mixtures listed in computer-output format (43 pages). In this data file, the molar volumes are expressed as polynomial functions of composition and temperature by a least-squares method. Four significant figures are given for molar volume and temperature. The units used in the file are $\text{cm}^3 \text{ mol}^{-1}$ for molar volume and K for temperature. Ordering information is given on any current masthead page.

Liquid-Liquid-Vapor Phase Equilibria of the Binary System Carbon Dioxide + *n*-Tridecane

David J. Fall and Kraemer D. Luks*

Department of Chemical Engineering, The University of Tulsa, Tulsa, Oklahoma 74104

The binary mixture carbon dioxide + *n*-tridecane is studied as a system exhibiting liquid-liquid-vapor equilibria. Pressure, temperature, and molar volumes and compositions of the two liquid phases are reported for a heretofore undetected second liquid-liquid-vapor locus, making this binary mixture a type IV system in the classification of van Krevelen and Scott. This second locus extends from a lower critical end point ($L = L-V$) at 310.8 K and 81.1 bar to an upper critical end point ($L-L = V$) at 313.9 K and 87.2 bar. A discussion on the evolution of the liquid-liquid-vapor equilibria in the homologous series of carbon dioxide + *n*-paraffin binary mixtures is presented.

Introduction

We have undertaken a detailed study of the multiphase equilibria behavior of CO_2 + hydrocarbon mixtures. Specific attention has recently been directed by us to the liquid-liquid-vapor (LLV) phase equilibria behavior of the homologous series of binary CO_2 + *n*-paraffin mixtures. These binary mixtures are important constituent pairs in CO_2 + crude oil systems as en-

countered in CO_2 -enhanced recovery processes. These "natural" multicomponent systems (1, 2) have been known to exhibit LLV immiscibility, and it has become apparent that hydrocarbon species of size *n*-heptane and larger are responsible for generating that immiscibility.

LLV immiscibility has been observed in a number of CO_2 + *n*-paraffin binary mixtures: *n*-heptane (3), *n*-octane (4-7), *n*-decane (8), *n*-undecane (5-7), *n*-dodecane (9), *n*-tridecane (5-7, 9), *n*-tetradecane (9), *n*-pentadecane (9), *n*-hexadecane (5-7), *n*-nonadecane (10), *n*-eicosane (10, 11), and *n*-heneicosane (10). Reference 3 demonstrated that *n*-heptane is the first of the *n*-paraffin homologous series to exhibit LLV immiscibility with CO_2 , while ref 10 identified *n*-heneicosane as the highest member of the series to do so.

It has been generally held that the LLV loci in this series of binary mixtures has been of two types, topographically speaking. For the hydrocarbons *n*-heptane to *n*-tridecane, the LLV locus has evolved from the solid-liquid-vapor (SLV) locus bounding the low-pressure end of the LV region, with its lower end point being a quadruple point (Q point, or four-phase point, SLLV) and its upper end point being a critical end point with liquid-liquid criticality ($L = L-V$). Hottovy et al. (9) reported that a change occurs in the nature of that LLV locus between *n*-

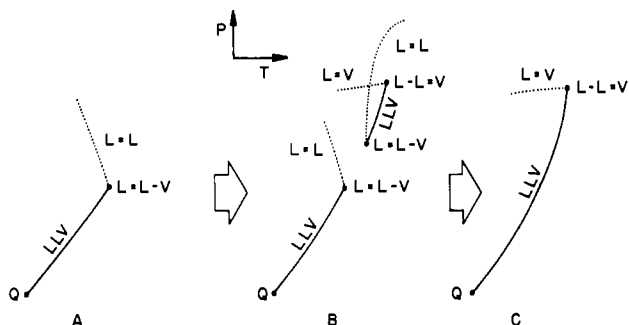


Figure 1. Schematic diagram in pressure-temperature space of the evolution of LLV behavior in the homologous series of $\text{CO}_2 + n$ -paraffin mixtures as carbon number increases.

tridecane and n -tetradecane, with the series from n -tetradecane to n -heneicosane exhibiting a locus with a Q-point (SLLV) lower terminus and a critical end point upper terminus having liquid-vapor criticality ($L = L = V$). This upper critical end point (K point) interrupts the locus of critical points $L = V$ which would normally run between the critical points of the two pure components constituting the binary mixture.

In certain instances, one can have two separate LLV locus branches for a binary mixture. The lower branch, having evolved from the SLV locus, is as described earlier, extending from a Q point to an upper critical end point $L = L - V$. The upper branch, with two critical end points, upper ($L = L = V$) and lower ($L = L - V$), evolves from the critical locus connecting the two pure-component critical points. This complex system might be expected to be an intermediate type of behavior between the binary systems with only the lower LLV locus, extending from Q(SLLV) to an $L = L - V$ point, and those with a single locus extending from Q(SLLV) to an $L = L = V$ point, or K point.

Figure 1 is an illustration of the evolution of LLV behavior that one might expect as carbon number increases in the homologous series of $\text{CO}_2 + n$ -paraffin binary mixtures from n -heptane to n -heneicosane. Detailed discussions of the various different types of binary phase equilibria behavior have been constructed by van Konynenburg and Scott (12) and Luks and Kohn (13).

With the scheme of Figure 1 for LLV behavior in mind, the investigators sought to find out whether there actually is a member of the $\text{CO}_2 + n$ -paraffin homologous series exhibiting the behavior of diagram B. An obvious candidate would be the binary mixture $\text{CO}_2 + n$ -tridecane. We report herein that such behavior is found for $\text{CO}_2 + n$ -tridecane, while no second LLV locus branch was found for the binary mixture $\text{CO}_2 + n$ -dodecane. Thus, the systems $\text{CO}_2 + n$ -heptane to n -dodecane are represented by diagram A in Figure 1. Diagram C represents the systems $\text{CO}_2 + n$ -tetradecane to n -heneicosane.

Experimental Apparatus and Procedures

A detailed description of the experimental apparatus is given in an earlier paper by us.¹⁰ The procedure for performing LLV studies is presented in another paper by us.¹⁴ Briefly summarizing those procedures, for an LLV study, a known amount of n -tridecane was placed in a 7.5-mL visual (glass) equilibrium cell. During an experimental run, measured amounts of CO_2 gas were added to the thermostated visual cell from a high-pressure bomb by means of a manual (Ruska) pump. By a careful mass balance, the moles of CO_2 in the liquid phases can be determined by "conjugate" measurements at a given temperature (the vapor phase is assumed to be pure CO_2 due to the low volatility of the n -tridecane at the temperatures of interest). Conjugate measurements involve two experimental runs in which one measurement has a large amount of L_1 relative to L_2 present (" L_1 -dominant") and the second measurement has $L_2 \gg L_1$ (" L_2 -dominant"). Lever principles (mass

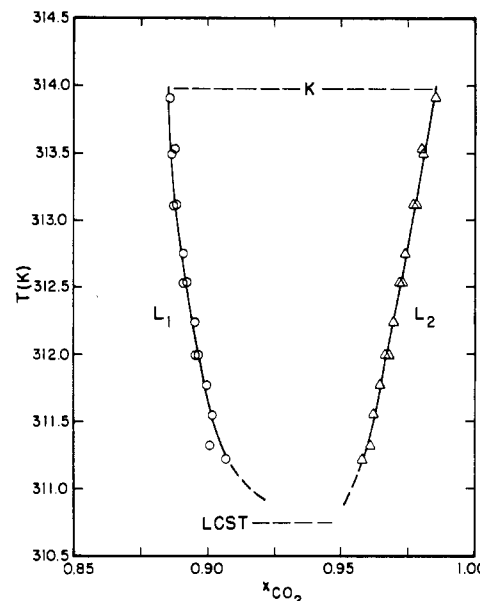


Figure 2. Composition as a function of temperature for the L_1 and L_2 phases for the upper branch of the LLV locus of $\text{CO}_2 + n$ -tridecane.

balances) can be applied so that compositions and molar volumes of L_1 and L_2 can be computed. The equations that result from the lever principle analysis are presented elsewhere (Appendix A, ref 14). The termination points of the LLV loci were determined individually by straightforward visual observation.

Temperature was measured with a Pt-resistance thermometer to an estimated accuracy of ± 0.02 K while pressure was measured to ± 0.07 bar (1 psia) with pressure transducers which were frequently calibrated against an accurate dead-weight gauge. Phase volumes in the calibrated visual cell were determined by a cathetometer to an accuracy of ± 0.005 mL.

Materials

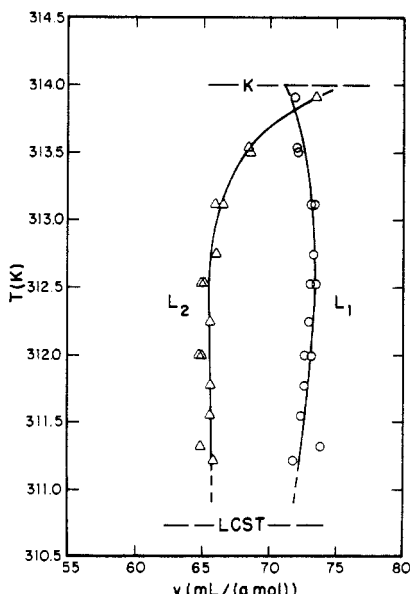
The n -tridecane was purchased from Alfa Products with a stated purity of 99 mol % and was used without further purification. Melting point depression analysis indicates this stated purity to be correct. The CO_2 was obtained from Air Products and Chemicals, Inc. as "Coleman Grade" with a purity rating of 99.99 mol %. The CO_2 was transferred to an initially evacuated storage bomb as a liquid at about 0 °C. In this two-phase condition, the vapor phase was vented and discarded to remove light gas impurities. Samples of the remaining CO_2 were liquefied in the visual cell at 25.00 °C and the pressure difference in the bubble and dew points was observed. This procedure generally produced a CO_2 supply with a pressure difference ranging from 0.5 to 2.0 psi. The vapor pressure at 25.00 °C and the critical temperature and pressure agreed with the literature values (15) to within ± 0.07 bar (1 psia) and ± 0.06 K, which is within the experimental accuracy of the visual cell technique in question for determining the location of a pure-component critical point.

Results

Table I presents raw data for the liquid-phase composition and molar volume for each of the liquid phases for the system $\text{CO}_2 + n$ -tridecane along the upper branch of its LLV locus. Figure 2 shows the liquid-phase compositions plotted against temperature; Figure 3 is a plot of temperature vs. the molar volumes of the two liquid phases. For all of these raw data, it is assumed that the gas phase is pure CO_2 . The temperatures should be good to ± 0.02 K for the LLV equilibria. All pressures are estimated to be good to ± 0.07 bar (1 psia). The mole fractions reported should be good to ± 0.001 while the molar volumes should be good to ± 0.8 mL/g-mol. These es-

Table I. Raw Data for the LLV Locus of the Binary System $\text{CO}_2 + n\text{-Tridecane}$

temp, K	press., bar	L ₁ phase		L ₂ phase	
		mole fraction of carbon dioxide	molar vol, mL/(g-mol)	mole fraction of carbon dioxide	molar vol, mL/(g-mol)
310.75	81.14 ^a				
311.21	81.92	0.9071	71.8	0.9578	65.8
311.32	82.30	0.9009	73.8	0.9608	64.8
311.55	82.53	0.9021	72.4	0.9621	65.6
311.77	82.92	0.8998	72.4	0.9646	65.6
311.99	83.48	0.8955	73.2	0.9681	64.7
311.99	83.54	0.8963	72.6	0.9668	64.9
312.24	83.78	0.8951	72.9	0.9695	65.6
312.53	84.49	0.8904	73.5	0.9732	65.1
312.53	84.50	0.8918	73.0	0.9723	65.0
312.75	84.71	0.8908	73.3	0.9739	65.8
313.11	85.54	0.8878	73.1	0.9781	66.5
313.11	85.58	0.8877	73.3	0.9773	65.8
313.49	86.30	0.8869	72.0	0.9809	68.6
313.54	86.18	0.8876	72.0	0.9805	68.4
313.91	86.92	0.8857	71.8	0.9852	73.4
313.94	87.24 ^b				
314.01	87.16 ^b				

^aLCST (L = L-V). ^bK point (L-L = V).**Figure 3.** Molar volume as a function of temperature for the L₁ and L₂ phases for the upper branch of the LLV locus of $\text{CO}_2 + n\text{-tridecane}$.

imates are based on the average absolute deviations of the LLV raw data from the smoothed curves shown in Figures 2 and 3. The AAD for the compositions of L₁ and L₂ are 0.0007 and 0.0005, respectively, while the AAD for the molar volumes of both L₁ and L₂ is 0.4 mL/g-mol.

The temperature-pressure locations of the critical end points (LCST and K points) in Table I are by their nature characterized by greater uncertainties than points along the LLV locus. The critical end points should be good to ± 0.05 K and ± 0.1 bar.

Remarks

Referring back to Figure 1, it appears that the homologous series of binary mixtures $\text{CO}_2 + n\text{-paraffins}$ exhibit LLV immiscibility with the following patterns: *n*-heptane to *n*-dodecane, Figure 1A; *n*-tridecane, Figure 1B; *n*-tetradecane to *n*-heneicosane, Figure 1C. In this present paper, only data on the upper branch of the LLV locus are reported; data on the lower branch were previously reported in ref 9. Table II lists the termination points of the LLV loci of several $\text{CO}_2 + n\text{-paraffin}$ binary mixtures. Noteworthy features of the series are the growth of the loci represented by Figure 1A with increasing

Table II. Temperatures (K) of End Points for the LLV Immiscibility Loci for Various Binary Mixtures of CO_2 and *n*-Paraffins

system	Q pt	UCST pt	LCST pt	K pt	ref
$\text{CO}_2 + n\text{-C}_7$	215.9	222.6			3
$\text{CO}_2 + n\text{-C}_8$	215.95	231.49			4
$\text{CO}_2 + n\text{-C}_{10}$	235.66	248.75			8
$\text{CO}_2 + n\text{-C}_{12}$	254.28	267.31			9
$\text{CO}_2 + n\text{-C}_{13}$	255.16	278.95	310.61 ^a	313.91 ^a	9
$\text{CO}_2 + n\text{-C}_{14}$	269.10			311.15	9
$\text{CO}_2 + n\text{-C}_{15}$	270.40			309.41	9
$\text{CO}_2 + n\text{-C}_{19}$	292.88			305.49	10
$\text{CO}_2 + n\text{-C}_{20}$	300.33			305.24	10
$\text{CO}_2 + n\text{-C}_{21}$	301.51			304.97	10

^aThis study.

carbon number up to 13, and the shortening of the loci represented by Figure 1C with increasing carbon number as one approaches carbon number 21. This latter phenomenon is caused by the increasing triple point temperatures of the *n*-paraffins, as it is the intersection of the SLV locus evolving out of the triple point of the *n*-paraffin with the LLV locus that forms the Q-point terminus (14). For carbon number 22 and higher the triple point of the *n*-paraffin is too high in temperature to have the related SLV locus pass below the (potential) K point at about 305 K.

The task of obtaining precise data for this binary system was made more difficult than in earlier LLV locus studies by the nature of this particular LLV locus. This upper LLV locus branch is only 3.3 K in extent and is terminated at both ends by critical end points. At the lower end, L₁ and L₂ are critical while at the upper end L₂ and V are critical. The effect is that along nearly all the locus branch certain phases are near-critical, with the attendant dilation which can cause rapid changes in composition and especially molar volume. Special care was taken by the investigators to ensure that the bath temperature of the experiment at any data point was stabilized for a substantial period of time so that the visual cell temperature was identifiable as precisely as possible, since the phase properties were such sensitive functions of state.

The problem of precision was further complicated by the fact that the properties of L₁ and L₂ are similar (as would be expected); the lever principles that are employed to compute the properties of the L₁ and L₂ phases from the laboratory data work best when the L₁ and L₂ phases differ widely in their properties (14).

Registry No. CO₂, 124-38-9; tridecane, 629-50-5.

Literature Cited

- (1) Orr, F. M.; Yu, A. D.; Lien, C. L. *Soc. Pet. Eng. J.* 1981, 480-92.
- (2) Turek, E. A.; Metcalfe, R. S.; Yarborough, L.; Robinson, R. L., paper SPE 9231 presented at the SPE 1980 Technical Conference and Exhibition, Dallas, TX Sept 21-24, 1980.
- (3) Im, V. K.; Kurata, F. *J. Chem. Eng. Data* 1971, 16, 412-5.
- (4) Hottovy, J. D.; Luks, K. D.; Kohn, J. P. *J. Chem. Eng. Data* 1982, 27, 298-302.
- (5) Schnelder, G.; Alwani, Z.; Helm, W.; Horvath, E.; Franck, E. *Chem.-Ing.-Tech.* 1967, 39, 649-56.
- (6) Schnelder, G. *Chem. Eng. Prog. Symp. Ser.* 1968, 64, 9-15.
- (7) Schnelder, G. *Adv. Chem. Phys.* 1970, 17, 1-42.
- (8) Kulkarni, A. A.; Zarab, B. Y.; Luks, K. D.; Kohn, J. P. *J. Chem. Eng. Data* 1974, 19, 92-4.
- (9) Hottovy, J. D.; Luks, K. D.; Kohn, J. P. *J. Chem. Eng. Data* 1981, 26, 256-8.
- (10) Fall, D. J.; Luks, K. D. *J. Chem. Eng. Data* 1984, 29, 413-7.
- (11) Hule, N. C.; Luks, K. D.; Kohn, J. P. *J. Chem. Eng. Data* 1973, 18, 311-3.
- (12) Van Konynenburg, P. H.; Scott, R. L. *Philos. Trans. R. Soc. London, Ser. A* 1980, 298, 495-540.
- (13) Luks, K. D.; Kohn, J. P. In "Proceedings of the 63rd Annual Convention, Gas Processors Association, New Orleans, LA, March 21, 1984"; Gas Processors Association: Tulsa, OK, 1984; pp 181-8.
- (14) Fall, D. J.; Fall, J. L.; Luks, K. D. *J. Chem. Eng. Data* 1985, 30, 82-8.
- (15) Vargaftik, N. B. "Tables on the Thermophysical Properties of Liquid and Gases", 2nd ed.; Wiley: New York, 1975; pp 167-8.

Received for review July 30, 1984. Accepted November 5, 1984. Support for this research was provided by the National Science Foundation (Grant No. CPE-8100450). The apparatus used is part of the PVTx laboratory at The University of Tulsa and was purchased with funds provided by several industries, The University of Tulsa, and a National Science Foundation specialized equipment grant (No. CPE-8014650).

Solubility of Octacalcium Phosphate at 25 and 45 °C in the System $\text{Ca(OH)}_2\text{-H}_3\text{PO}_4\text{-KNO}_3\text{-H}_2\text{O}$

J. C. Heughebaert[†] and G. H. Nancollas*

Chemistry Department, State University of New York at Buffalo, Buffalo, New York 14214

The solubility product of octacalcium phosphate ($\text{Ca}_4\text{H}(\text{PO}_4)_3\cdot2.25\text{H}_2\text{O}$) has been determined in the system $\text{Ca(OH)}_2\text{-H}_3\text{PO}_4\text{-KNO}_3\text{-H}_2\text{O}$ at 25 and 45 °C by allowing both growth and dissolution experiments over a range of ionic strength to come to equilibrium. Values of $pK_{\infty} = 49.6 \pm 0.2$ and 49.8 ± 0.3 , respectively, were obtained by taking into account activity coefficient corrections and ion-pair formation.

Introduction

Octacalcium phosphate ($\text{Ca}_4\text{H}(\text{PO}_4)_3\cdot2.5\text{H}_2\text{O}$, hereafter OCP) is one of the most important calcium phosphate phases since it has been implicated as a precursor to the formation of hydroxyapatite ($\text{Ca}_5(\text{PO}_4)_3\text{OH}$, hereafter HAP), in biological mineralization (1, 2). Although values of the solubility have been reported at 25 and 37 °C (3, 4), it was discovered that OCP could be grown in a range of solution composition which, on the basis of these data, would be expected to be undersaturated (5). A redetermination of the solubility at 37 °C indicated a value smaller than that previously reported and it was possible to demonstrate the crystallization of pure OCP within the pH range 6-7 (6). The unusually large difference between the solubilities at 25 and 37 °C in the literature prompted us to redetermine the values at other temperatures and to ensure the stability of the OCP phase by allowing both growth and dissolution experiments to come to equilibrium.

Experimental Section

Deionized, triply distilled water purged with presaturated nitrogen gas to exclude carbon dioxide was used to prepare solutions. Potassium hydroxide was prepared from Dilutit reagents (J. T. Baker Co.) and was standardized against potassium hydrogen phthalate (J. T. Baker Co.) by using both potentiometric and colorimetric (thymolphthalein blue) titrations. Stock solutions of calcium nitrate (Ventron Co. Alfa Division) potassium dihydrogen phosphate (J. T. Baker Co.) and potassium nitrate (Ventron Co. Alfa Division) were prepared from the

ultrapure-grade salts. Analyses for calcium and potassium ions in these stock solutions were made by passing aliquots through Dowex 50W-XB ion-exchanger columns in the hydrogen form and titrating the eluted acid against potassium hydroxide solution.

The OCP sample was prepared by using the constant-composition crystallization method at a pH of 6.0 (6). The solid phase was filtered through a 0.2-μm filter (Millipore, Bedford, MA) and X-ray powder diffraction (XRD 3000 Phillips diffractometer, Cu Kα radiation, Ni filter) gave no evidence of any phase other than OCP. Calcium and phosphate were analyzed by using absorption spectroscopy (Perkin-Elmer Model 503) for calcium and spectrophotometry (Varian Model Cary 210) for phosphate (7). Chemical analysis of the OCP preparation gave a molar calcium/phosphate ratio of $1.33_8 \pm 0.01$. The specific surface area of the crystals, $9.0 \pm 0.2 \text{ m}^2 \text{ g}^{-1}$, was determined by a single-point BET method (70/30, He/N₂ gas mixture, Quanta-sorb, Quantachrome, Greenvale, NY).

The solubility of OCP was determined by allowing OCP crystal growth and dissolution experiments to proceed to equilibrium in solutions initially supersaturated or undersaturated with respect to OCP. Approximately 30 mg of crystals was added to 100 mL of solutions containing calcium nitrate, potassium dihydrogen phosphate, and potassium nitrate at a pH of 6.2. The suspensions were sealed in Pyrex vessels and shaken in a thermostat at 25 or 45 °C. Equilibrations were allowed to proceed for 28 days at 25 °C and 12 days at 45 °C using different conditions of stirring, initial concentrations, and ionic strength. At the end of these time periods the pH was measured by using a glass electrode (Beckmann Instruments) and a silver/silver chloride reference electrode. The latter incorporated an intermediate liquid junction containing potassium chloride solution at the same ionic strength as the solution being studied. For the calcium and phosphate determinations, care was taken to use standard solutions of the same ionic composition as the test media. It was important to verify, by chemical analysis, X-ray diffraction, and infrared spectroscopy, the absence of solid phases other than OCP in the experiments.

Results and Discussion

The concentrations of ionic species in the equilibrated calcium phosphate solutions were calculated by using expressions

[†]Laboratoire de Physico-Chimie des Solides, ERA CNRS No. 263, 31400 Toulouse, France.